LONG-TERM PERSISTENCE OF THE PASSIVE FILM ON ALLOY 22 AT ELEVATED TEMPERATURES IN THE POTENTIAL YUCCA MOUNTAIN REPOSITORY ENVIRONMENT

Prepared for

U.S. Nuclear Regulatory Commission
Contract NRC–02–07–006

Prepared by

H. Jung[1]
T. Mintz[1]
L. Yang[1]
T. Ahn[2]

[1]Center for Nuclear Waste Regulatory Analyses
San Antonio, Texas

[2]U.S. Nuclear Regulatory Commission
Washington, DC

January 2009

PREVIOUS REPORTS IN SERIES

Number	Number	Dates Issued
CNWRA 91-004	A Review of Localized Corrosion of High-Level Nuclear Waste Container Materials—I	April 1991
CNWRA 91-008	Hydrogen Embrittlement of Candidate Container Materials	June 1991
CNWRA 92-021	A Review of Stress Corrosion Cracking of High-Level Nuclear Waste Container Materials—I	August 1992
CNWRA 93-003	Long-Term Stability of High-Level Nuclear Waste Container Materials: I—Thermal Stability of Alloy 825	February 1993
CNWRA 93-004	Experimental Investigations of Localized Corrosion of High-Level Nuclear Waste Container Materials	February 1993
CNWRA 93-006	Characteristics of Spent Nuclear Fuel and Cladding Relevant to High-Level Waste Source Term	May 1993
CNWRA 93-014	A Review of the Potential for Microbially Influenced Corrosion of High-Level Nuclear Waste Containers	June 1993
CNWRA 94-010	A Review of Degradation Modes of Alternate Container Designs and Materials	April 1994
CNWRA 94-028	Environmental Effects on Stress Corrosion Cracking of Type 316L Stainless Steel and Alloy 825 as High-Level Nuclear Waste Container Materials	October 1994
CNWRA 95-010	Experimental Investigations of Failure Processes of High-Level Radioactive Waste Container Materials	May 1995
CNWRA 95-020	Expert-Panel Review of the Integrated Waste Package Experiments Research Project	September 1995
CNWRA 96-004	Thermal Stability and Mechanical Properties of High-Level Radioactive Waste Container Materials: Assessment of Carbon and Low-Alloy Steels	May 1996
CNWRA 97-010	An Analysis of Galvanic Coupling Effects on the Performance of High-Level Nuclear Waste Container Materials	August 1997
CNWRA 98-004	Effect of Galvanic Coupling Between Overpack Materials of High-Level Nuclear Waste Containers—Experimental and Modeling Results	March 1998

PREVIOUS REPORTS IN SERIES (continued)

Number	Number	Dates Issued
CNWRA 98-008	Effects of Environmental Factors on Container Life	July 1998
CNWRA 99-003	Assessment of Performance Issues Related to Alternate Engineered Barrier System Materials and Design Options	September 1999
CNWRA 99-004	Effects of Environmental Factors on the Aqueous Corrosion of High-Level Radioactive Waste Containers—Experimental Results and Models	September 1999
CNWRA 2000-06 Revision 1	Assessment of Methodologies To Confirm Container Performance Model Predictions	January 2001
CNWRA 2001-003	Effect of Environment on the Corrosion of Waste Package and Drip Shield Materials	September 2001
CNWRA 2002-01	Effect of In-Package Chemistry on the Degradation of Vitrified High-Level Radioactive Waste and Spent Nuclear Fuel Cladding	October 2001
CNWRA 2002-02	Evaluation of Analogs for the Performance Assessment of High-Level Waste Container Materials	March 2002
CNWRA 2003-01	Passive Dissolution of Container Materials—Modeling and Experiments	October 2002
CNWRA 2003-02	Stress Corrosion Cracking and Hydrogen Embrittlement of Container and Drip Shield Materials	October 2002
CNWRA 2003-05	Assessment of Mechanisms for Early Waste Package Failures	March 2003
CNWRA 2004-01	Effect of Fabrication Processes on Materials Stability—Characterization and Corrosion	October 2003
CNWRA 2004-02	Natural Analogs of High-Level Waste Container Materials—Experimental Evaluation of Josephinite	January 2004
CNWRA 2004-03	The Effects of Fabrication Processes on the Mechanical Properties of Waste Packages—Progress Report	July 2004
CNWRA 2004-08	A Review Report of High Burnup Spent Nuclear Fuel—Disposal Issues	September 2004
CNWRA 2005-01	Microbially Influenced Corrosion Studies of Engineered Barrier System Materials	October 2004

PREVIOUS REPORTS IN SERIES (continued)

Number	Number	Dates Issued
CNWRA 2005-02	Passive and Localized Corrosion of Overpack Materials—Modeling and Experiments	November 2005
CNWRA 2005-03	Microstructural Analyses and Mechanical Properties of Alloy 22	March 2005
CNWRA 2006-01	Crevice Corrosion Penetration Rates of Alloy 22 in Chloride-Containing Waters—Progress Report	December 2005
CNWRA 2006-02	Corrosion of Alloy 22 in Concentrated Nitrate and Chloride Salt Environments at Elevated Temperatures—Progress Report	April 2006
CNWRA 2007-01	Stress Corrosion Cracking of Waste Package Material—Modeling and Experiments	December 2006

ABSTRACT

This report documents an evaluation of the long-term persistence of the passive film on Alloy 22 (Ni-22Cr-13Mo-4Fe-3W) at elevated temperatures {e.g., above 100 °C [212 °F]}. Two areas are evaluated: (i) passive film stability with respect to composition and structure and (ii) the effects of anodic sulfur segregation on stability.

Thermodynamic modeling of Alloy 22 in simulated concentrated water at temperatures of 150 °C [302 °F] and 180 °C [356 °F] indicates that there is a large range of conditions where a chromium-rich oxide would be present on an Alloy 22 surface. Under very acidic waters or at high potentials, the thermodynamic results indicate that the chromium-rich oxide is unstable. Short-term corrosion test results for Alloy 22 above 120 °C [248 °F] reported in the literature revealed that a chromium-rich oxide film was present in most testing conditions, which is consistent with the thermodynamic results. This chromium oxide was mainly in the +3 oxidation state, which would be either Cr_2O_3, $Cr(OH)_3$, CrOOH, or possibly $NiCr_2O_4$. At much higher temperatures {at least 160 °C [320 °F]} and high nitrate-to-chloride ratio (roughly 7.4), the chromium oxidized to the +6 state, which would be expected to more readily dissolve. An additional review of analog materials (Alloys 600 and 690) demonstrated that a passive chromium-rich oxide film can form at elevated temperature in various pHs.

Preliminary experiments conducted at the Center for Nuclear Waste Regulatory Analyses (CNWRA®) suggest that sulfur in Alloy 22 (maximum 200 ppm in weight, in general) could accumulate on the alloy surface. Windisch, et al. (2007) reported a 2 to 5 percent increase in sulfur concentration on the surface of Alloy 22 in a 29-day test conducted in 1 M NaCl solution at room temperature. The sulfur accumulation observed in the CNWRA test was limited {e.g., less than a monolayer of sulfur, about 40 nanogram/cm^2 [1.4×10^{-11} lb/in^2]}. This may be due to the presence of alloying elements (i.e., chromium and molybdenum), which counteract potential detrimental effects of sulfur segregation. Thermodynamic calculations conducted in the present study predict a formation of stable chromium oxide and possible soluble molybdenum sulfide at elevated temperatures {e.g., 150 °C [302 °F]} under a wide range of potential and pH, indicating sulfur segregation may not be an issue. It may be possible to explain greater sulfur accumulation reported in some of the literature by considering kinetic aspect associated with the sulfur segregation process. CNWRA conducted scratch repassivation tests to evaluate the repassivation capability of Alloy 22 under sulfur segregation simulated conditions. The passive film was mechanically disrupted by scratching the alloy surface in sulfur-containing solutions. The results show that Alloy 22 repassivated within a few seconds in chloride solutions (0.5 M NaCl and simulated concentrated water) containing various concentrations of sulfide at 22 and 60 °C [71.6 and 140 °F]. Therefore, as long as the beneficial roles of chromium and molybdenum in Alloy 22 to counteract the potential detrimental sulfur effects at high temperature are not different from those at low temperatures, sulfur segregation may not have any significant detrimental effect on the long-term passive film stability of Alloy 22.

Reference

Windisch Jr., C.F., D.R. Baer, R.H. Jones, and M.H. Engelhard. "Electrochemical Effects of S Accumulation on Ion-Implanted Alloy 22 in 1 M NaCl Solutions." *Corrosion Science*. Vol. 49. pp. 2,497–2,511. 2007.

CONTENTS

CONTENTS (continued)

FIGURES

TABLES

EXECUTIVE SUMMARY

The potential waste package design (DOE, 2002) may include an outer container constructed of Alloy 22, a corrosion-resistant Ni-22Cr-13Mo-4Fe-3W alloy that is highly resistant to various modes of corrosion including dry-air oxidation, general corrosion, localized corrosion, and stress corrosion cracking. In the absence of an environment leading to localized corrosion, Alloy 22 is expected to corrode uniformly with very low corrosion rates under the potential repository conditions (Dunn, et al., 2005; Pensado, et al., 2002).

Low rates of general corrosion are predicated based on the stability of the passive film that is expected to form on Alloy 22. Loss of passivity could lead to general corrosion rates that are orders of magnitude higher than those corresponding to passive dissolution, resulting in shorter waste package lifetimes and potential release of radionuclides. For this reason, the long-term persistence of the passive film on Alloy 22 is considered to be of high risk significance to waste isolation relative to other corrosion modes (NRC, 2005).

Previously, the long-term persistence of the passive film on Alloy 22 at relatively low temperatures {less than 100 °C [212 °F]} was analyzed based on the short-term corrosion test data from literature (Jung, et al., 2007). It was concluded that short-term passivity can be maintained at low temperatures under conditions representative of the potential repository. No specific degradation mechanisms were observed to interfere with the stability of a passive film over the short testing periods. Several corrosion-related degradation processes that may affect a long-term persistence of the passive film on Alloy 22 were evaluated, including enhanced corrosion rate by anodic sulfur segregation, detrimental effects of base metal chromium depletion at the metal–film interface, film spallation by void formation, anion-selective sorption, increased cathodic kinetics, and alteration of passivation by dry–wet cyclic processes. Among these processes, enhanced corrosion rate by anodic sulfur segregation was identified as being potentially detrimental and requiring further experimental evaluation. Other degradation processes Jung, et al. (2007) considered did not appreciably affect the long-term stability of the passive film on Alloy 22.

This report focuses on the long-term persistence of the passive film on Alloy 22 at elevated temperatures {e.g., above 100 °C [202 °F]} and the possible detrimental effect of sulfur segregation on Alloy 22 passive film stability in the potential Yucca Mountain repository environment. The present work (i) assesses the passive film stability and evolution of film thickness, composition, and structure at elevated temperatures and (ii) evaluates the effects of anodic sulfur segregation on the long-term persistence of the passive film on Alloy 22 through scoping corrosion tests.

Thermodynamic modeling of Alloy 22 in simulated concentrated water at temperatures of 150 and 180 °C [302 and 356 °F] was conducted to examine the passive film stability. The pH-potential diagrams showed a large region of stability for either Cr_2O_3 and/or $NiCr_2O_4$. Both of these compounds contain chromium in the +3 state, which is consistent with the experimental data reported in literature. At very acidic or high potentials, the thermodynamic results suggest that the chromium-rich oxide tends to be unstable. An examination of short-term autoclave testing for Alloy 22 at elevated temperatures (Orme, et al., 2004) indicated that a chromium-rich oxide film was present in most of the testing conditions. This chromium oxide was mainly in the +3 oxidation state, which would be either Cr_2O_3, $Cr(OH)_3$, CrOOH, or possibly $NiCr_2O_4$. At much higher temperature {at least 160 °C [320 °F]} and high nitrate-to-chloride ratio (roughly 7.4), the chromium oxidized to the +6 state, which would be expected to more readily dissolve. An

additional literature review of chromium-containing nickel alloys (e.g., Alloys 600 and 690) is consistent with the notion that a passive chromium-rich oxide film can form at elevated temperatures {e.g., above 100 °C [212 °F]} in a range of pH (Montemor, et al., 2003; Hur and Park, 2006; Mintz and Devine, 2004).

The potential deleterious effects of anodic sulfur segregation on the passive film stability of Alloy 22 were evaluated by thermodynamic calculations and scoping corrosion tests. The experimental work in this study suggests that sulfur in Alloy 22 (maximum 200 ppm in weight) could accumulate on the alloy surface by anodic sulfur segregation. However, the amount of the accumulated sulfur was limited {e.g., a monolayer of sulfur, about 40 nanogram/cm^2 [1.4 × 10^{-11} lb/in^2]} due to the presence of alloying elements (i.e., chromium and molybdenum), which counteract potential detrimental effects of sulfur segregation. In the literature, (Windisch, et al., 2007), the sulfur concentration on Alloy 22 was reported to increase 2 to 5 percent in 1 M NaCl solution immersion tests at room temperature after 29 days. Under the hypothesis of film breakdown due to sulfur segregation, the Center for Nuclear Waste Regulatory Analyses conducted scratch tests to evaluate the repassivation capability of Alloy 22 in sulfur-containing solutions. The scratch tests showed that Alloy 22 repassivated within a few seconds in chloride solutions containing various concentrations of sulfide (0.5 M NaCl and simulated concentrated water) at 22 and 60 °C [72 and 140 °F]. The corrosion test cell used for the scratch test was able to operate up to the maximum temperature of 60 °C [140 °F].

The thermodynamic calculations show that a stable insoluble chromium oxide and possible soluble molybdenum sulfides at 150 °C [302 °F] are present in a wide range of potentials and pH. Therefore, as long as the beneficial roles of alloying elements (i.e., chromium and molybdenum) are present, sulfur segregation may not have a significant detrimental effect on the passive film stability of Alloy 22 at elevated temperatures {e.g., above 100 °C [212 °F]}.

References

DOE. DOE/RW–0539–1, "Yucca Mountain Science and Engineering Report: Technical Information Supporting Site Recommendation Consideration." Rev. 1. Las Vegas, Nevada: DOE, Office of Civilian Radioactive Waste Management. 2002.

Dunn, D.S., O. Pensado, Y.-M. Pan, R.T. Pabalan, L. Yang, X. He, and K.T. Chiang. "Passive and Localized Corrosion of Alloy 22-Modeling and Experiments." CNWRA 2005-02. Rev. 1. San Antonio, Texas: CNWRA. 2005.

Hur, D.H. and Y.S. Park. "Effect of Temperature on the Pitting Behavior and Passive Film Characteristics of Alloy 600 in Chloride Solution." *Corrosion*. Vol. 62, No. 9. pp. 745–750. 2006.

Jung, H., T. Mintz, D.S. Dunn, O. Pensado, and T. Ahn. "A Review of the Long-Term Persistence of the Passive Film on Alloy 22 in Potential Yucca Mountain Repository Environments." ML072880595. Washington, DC: NRC. 2007.

Mintz, T.M. and T.M. Devine. "Influence of Surface Films on the Susceptibility of Inconel 600 to Stress Corrosion Cracking." *Key Engineering Materials.* Vols. 261–263. pp. 875–884. 2004.

Montemor, M.F., M.G.S Ferreira, M. Walls, B. Rondot, and M. Cunha Belo. "Influence of pH on Properties of Oxide Films Formed on Type 316L Stainless Steel, Alloy 600, and Alloy 690 in High-Temperature Aqueous Environments." *Corrosion*. Vol. 59, No. 1. pp. 11–21. 2003.

NRC. NUREG–1762, "Integrated Issue Resolution Status Report." Rev. 1. Appendix D. Washington, DC: NRC. April 2005.

Orme, C.A., J. Gray, J. Hayes, L. Wong, R. Rebak, S. Carroll, J. Harper, and G. Gdowski. "Fiscal Year 2004 Summary Report: General Corrosion and Passive Film Stability." UCRL–TR–208588. Livermore, California: Lawrence Livermore National Laboratory. 2004.

Pensado, O., D.S. Dunn, G.A. Cragnolino, and V. Jain. "Passive Dissolution of Container Materials-Modeling and Experiments." CNWRA 2003-01. San Antonio, Texas: CNWRA. 2002.

Windisch, Jr., C.F., D.R. Baer, R.H. Jones, and M.H. Engelhard. "Electrochemical Effects of S Accumulation on Ion-Implanted Alloy 22 in 1 M NaCl Solutions." *Corrosion Science*. Vol. 49. pp. 2,497–2,511. 2007.

ACKNOWLEDGMENTS

This report describes work performed by the Center for Nuclear Waste Regulatory Analyses (CNWRA®) and its contractors for the U.S. Nuclear Regulatory Commission (NRC) under Contract No. NRC–02–07–006. The activities reported here were performed on behalf of the NRC Office of Nuclear Material Safety and Safeguards, Division of High-Level Waste Repository Safety. This report is an independent product of CNWRA and does not necessarily reflect the view or regulatory position of NRC. The NRC staff views expressed herein are preliminary and do not constitute a final judgment or determination of the matters addressed or of the acceptability of a license application for a geologic repository at Yucca Mountain.

The authors gratefully acknowledge O. Pensado for his technical review, B. Sagar for his programmatic review, L. Mulverhill for her editorial review, and B. Street and J. Gonzalez for their administrative support. The authors also acknowledge K. Axler, Y.-M. Pan, and G. Cragnolino for their assistance throughout this project.

QUALITY OF DATA, ANALYSES, AND CODE DEVELOPMENT

DATA: All CNWRA-generated original data contained in this report meet the quality assurance requirements described in the Geosciences and Engineering Division Quality Assurance Manual. Sources for other data should be consulted for determining the level of quality for those data. Computational calculations have been recorded in CNWRA Scientific Notebooks 835 (Jung, 2008) and 900 (Jung and Ellis, 2008).

ANALYSES AND CODES: The computer software Corrosion Analyzer™ (OLI Systems, Inc., 2006) was used in the analyses contained in this report. Corrosion Analyzer is commercial software controlled under the CNWRA quality assurance procedure Technical Operating Procedure (TOP)–18. Documentation for thermodynamic calculation in Section 2.2 can be found in Scientific Notebook 923E (Mintz, 2008).

Reference

Jung, H. Scientific Notebook No. 835. pp. 20–27. San Antonio, Texas: CNWRA. 2008

Jung, H and C. Ellis. Scientific Notebook No. 900. pp. 20–33, 43, and 87–94. San Antonio, Texas: CNWRA. 2008.

Mintz, T. Scientific Notebook No. 923E. pp. 3–52. San Antonio, Texas: CNWRA. 2008.

OLI Systems, Inc. “Corrosion Analyzer Software.” Version 2.0. Morris Plains, New Jersey: OLI Systems, Inc. 2006.

1 INTRODUCTION

The U.S. Nuclear Regulatory Commission (NRC) is currently reviewing a U.S. Department of Energy (DOE) license application for construction and operation of a high-level nuclear waste repository at Yucca Mountain, Nevada, for the permanent disposal of high-level waste. Waste packages will be potentially emplaced in a series of drifts that will be mined, in parallel, in the unsaturated zone approximately 300 m [984 ft] below the surface and approximately 300 m [984 ft] above the water table.

One of the key attributes for the overall system performance of the potential repository is the long lifetime of waste packages as a barrier to radionuclide release (DOE, 2002). For nominal repository conditions, corrosion is considered to be an important factor in the potential degradation of the waste package. The reference waste package design in the DOE site recommendation (DOE, 2002) consists of an outer cylindrical container made of a highly corrosion-resistant nickel-based alloy, Alloy 22 (Ni-22Cr-13Mo-4Fe-3W), and an inner container of Type 316L nuclear grade SS (low C-high N-Fe-18Cr-12Ni-2.5Mo) to provide structural support.

Multiple investigations indicate that Alloy 22 is highly resistant to various modes of corrosion including dry-air oxidation, general (uniform) corrosion, localized corrosion, and stress corrosion cracking. Corrosion resistance is mainly due to the presence of a chromium-rich passive film formed on the alloy surface in a wide range of environments from oxidizing to reducing conditions in a range of pH and temperature. In the absence of environmental and materials conditions leading to localized corrosion or stress corrosion cracking, Alloy 22 is expected to corrode uniformly with very low corrosion rates in aqueous environments (Dunn, et al., 2005; Pensado, et al., 2002). Low general corrosion rates are dependent on passive film characteristics.

The passive film formed under aqueous solution consists of a multilayered structure with a chromium-rich inner layer and metal oxi-hydroxides on successive outer layers. According to the bilayer model (Macdonald, 1992, 1999; Marcus and Maurice, 2000), the passive film generally consists of a compact inner layer of oxide and a porous outer layer of hydroxide or oxy-hydroxide. The inner layer forms by solid state reactions, and it is mostly responsible for the phenomenon of passivity. The outer layer is believed to play only a secondary role in alloy passivation. If the passive film persists indefinitely, the general corrosion rates for Alloy 22 could be very low. For example, in a recent analysis (Leslie, et al., 2007) a waste package failure by general corrosion where passivity persists is estimated to occur well beyond 10,000 years.

Loss of passivity (i.e., depassivation) could lead to general corrosion rates that are orders of magnitude higher than those corresponding to passive dissolution. Certain aggressive water chemistries characterized by high chloride concentration, low pH, and high temperature may disrupt the Alloy 22 passive film. For example, Alloy 22 exhibited depassivation in concentrated brines [e.g., 18 m $CaCl_2$ with 0.9 m $Ca(NO_3)_2$] at 155 °C [311 °F] (Rodríguez, et al., 2007).

Radionuclide release depends in part on the extent of the opening area of the waste package surface. With a small restricted opening area, groundwater entry into the failed waste package likely will be of a small volume. The small volume of groundwater could mobilize and release a small amount of radionuclides from waste from dissolution. Corrosion modes such as crevice corrosion and stress corrosion cracking may induce a small opening from small crevice areas or tight cracks. However, passivity loss may induce a large opening area because general

corrosion by the passivity loss could occur on the total surface of the waste package. This large opening area could result in a relatively larger amount of radionuclide release than for corrosion modes with small area openings. For this reason, the long-term persistence of the passive film on Alloy 22 is considered to be of high risk significance to waste isolation (NRC, 2005).

After repository closure, the temperature at the waste package surfaces is expected to increase. DOE analyses estimate maximum temperatures of approximately 200 °C [392 °F] depending on factors such as the location of the waste package and spent fuel loading (Sandia National Laboratory, 2007a). Hence, aqueous solutions that potentially could contact hot waste package surfaces could evolve into brines either through evaporation of seepage water or by deliquescence of soluble salts in dusts that deposit on the waste package surfaces. Because of the high boiling points of solutions formed with NaCl-$NaNO_3$-KNO_3 salts, aqueous solutions may be present on the waste package surface during the high-temperature period after closure. Experiments conducted by the DOE suggest stable NaCl-$NaNO_3$-KNO_3 brines at temperatures up to 190 °C [374 °F] (Sandia National Laboratory, 2007b). The presence of brines is important because many metals have higher general corrosion rates or are more susceptible to localized corrosion at the elevated temperatures of aqueous systems that are possible in the presence of brines. Yang (2006) has reported general corrosion rates of Alloy 22 between 0.95 and 9.4 μm/yr [0.037 and 0.37 mil/yr] for the specimens immersed in nitrate-rich chloride containing brines (pH of ~2 to 4.3) at temperatures between 150 and 180 °C [302 and 356 °F].

The long-term persistence of the passive film on Alloy 22 at relatively low temperatures {less than 100 °C [212 °F]} was previously evaluated based on short-term corrosion test data from literature (Jung, et al., 2007). The literature survey supports the notion that passivity can be maintained at low temperatures for an extended period. No specific degradation mechanisms were identified to interfere with the stability of a passive film in short-term tests. Several corrosion-related degradation processes that may affect long-term persistence of the passive film on Alloy 22 were evaluated, including enhanced corrosion rate by anodic sulfur segregation, detrimental effects of base metal chromium depletion at the metal–film interface, film spallation by void formation, anion-selective sorption, increased cathodic kinetics, and alteration of passivation by dry–wet cyclic processes. Among these processes, enhanced corrosion rate by anodic sulfur segregation was identified as requiring further experimental evaluation. Other degradation processes Jung, et al. (2007) considered did not appreciably affect the long-term stability of the passive film on Alloy 22.

1.1 Objective and Scope

This report examines the long-term persistence of the passive film on Alloy 22 at elevated temperatures {e.g., above 100 °C [202 °F]}. The objectives of the present work are to (i) assess the passive film stability with respect to film composition and structure at elevated temperatures and (ii) evaluate the effects of anodic sulfur segregation on the long-term persistence of the passive film on Alloy 22 through scoping corrosion tests.

In assessing the long-term passive film stability of Alloy 22 at elevated temperature, the thermodynamic composition of the passive film on Alloy 22 at elevated temperature was modeled considering simulated concentrated water solutions at temperatures of 150 and 180 °C [302 and 356 °F]. The thermodynamic results were compared to short-term corrosion test data on Alloy 22 and analog materials from the open literature.

To evaluate the effects of anodic sulfur segregation, two different experimental approaches were used: a scratch repassivation technique and an electrochemically accelerated dissolution process. The scratch repassivation test investigated the repassivation capability of Alloy 22 when the passive film was mechanically disrupted by scratching the metal surface. Scratch repassivation tests were conducted in two different types of solutions (0.5 M NaCl and simulated concentrated water) containing dissolved sulfur species at temperatures of 22 and 60 °C [71.6 and 140 °F]. In the other approach, the anodic dissolution of Alloy 22 was accelerated electrochemically in a aggressive environment {i.e., 0.5 M HCl solutions, pH of 0.2 at 95 °C [203 °F]}. This accelerated corrosion test investigated whether sulfur in Alloy 22 can accumulate on the alloy surface. Thermodynamic stability of metal sulfides at elevated temperatures was examined by constructing the potential-pH diagrams for nickel-, chromium-and molybdenum-sulfur-water systems at 150 °C [302 °F].

1.2 Organization of the Report

This report is organized into four chapters to address the objective and scope identified in Section 1.1. Chapter 1 is an introduction. In Chapter 2, the nature and stability of the passive film that formed on the surfaces of Alloy 22 is discussed. Also, Chapter 2 includes a discussion of analog materials at elevated temperatures. The results of thermodynamic modeling in simulated concentrated water at 150 and 180 °C [302 and 356 °F] are also presented. The calculated temperature and relative humidity at the potential Yucca Mountain repository is briefly summarized as background information. In Chapter 3, the test results from scratch repassivation tests and accelerated corrosion tests are presented. Thermodynamic stability diagrams for nickel-, chromium-, and molybdenum-sulfur-water systems at 150 °C [302 °F] are also presented, and the results are discussed. An assessment of the potential effects of anodic sulfur segregation on the passive film stability of Alloy 22 in a potential repository environment is provided. Chapter 4 summarizes the main conclusions.

2 PASSIVE FILM STABILITY OF ALLOY 22 AT ELEVATED TEMPERATURES

Passivity occurs when an alloy forms a thin, protective passive film on its surface in aqueous solutions, significantly decreasing the general corrosion rate. Chromium-containing alloys form a very stable passive film. The structure and composition of the passive film is, in general, difficult to determine because passive films are typically only a few nanometers thick. The passive film is considered to have a bilayer structure. According to the bilayer model (Macdonald, 1999, 1992; Marcus and Maurice, 2000), the passive film generally consists of a compact inner layer of oxide and a porous outer layer of hydroxide or oxy-hydroxide. The inner layer is normally assumed to be a chromium-rich oxide that conforms to the surface of the base metal. An outer film is typically believed to be made up of nickel and iron oxide/hydroxide. The outer layer tends to form by dissolution and precipitation reactions. The outer layer may contribute to the overall low corrosion rate of the alloy, but the inner chromium-rich layer is usually considered to determine the passive state. Chromium-containing alloys are considered to form a very stable passive film.

As mentioned previously, the passive film has been directly related to the corrosion resistance of the alloy. The long-term stability of the passive film formed on Alloy 22 can be evaluated by conducting temperature-dependent measurements of its thickness, composition, and structure. U.S. Department of Energy (DOE) estimated the maximum temperatures at the waste package surface to be on the order of ~200 °C [392 °F] (Sandia National Laboratory, 2007a).

This chapter reviews current literature on the experimental properties and composition of the passive film on both Alloy 22 and two analog materials (i.e., Alloys 600 and 690) at elevated temperatures {> 100 °C [212 °F]}. Choosing to evaluate these analog materials to understand the passive nature of Alloy 22 is reasonable because the chromium concentration in Alloys 600 and 690 envelops the chromium content of Alloy 22. This chapter examines how the passive film on Alloy 22 may change with temperature utilizing thermodynamic modeling in simulated concentrated water at temperatures of 150 and 180 °C [302 and 356 °F]. Finally, passive film stability of Alloy 22 at the potential repository environment is discussed.

2.1 Temperature and Relative Humidity Conditions at the Potential Repository

After the end of the ventilation period and repository closure, the temperature of the waste package initially rises, reaching a peak temperature at about 40 years, followed by a gradual cooling (Sandia National Laboratories, 2007a). Drift and waste package temperatures will depend on many factors such as the heat-generation rate, ventilation before permanent closure, and conductivity of the host rock. In addition, these calculations consider the orientation and distance between neighboring drifts allowing for thermal interactions. As a result, the drifts near the edges of the repository are estimated to have lower temperatures than those in the center of the repository and the temperature at the end of the drifts is estimated to be lower than that at the center. Another factor that may affect the temperature is related to drift degradation, which may lead to rubble accumulation on the drip shield and influence the effective thermal insulation (Fedors, et al., 2004). Figures 2-1 and 2-2 show the calculated ranges of temperature and relative humidity versus time for three distinct waste packages, respectively, including a cool defense high-level waste package at the edge of the repository, an average commercial boiling water reactor waste package at the center of the repository, and a thermally hot pressurized

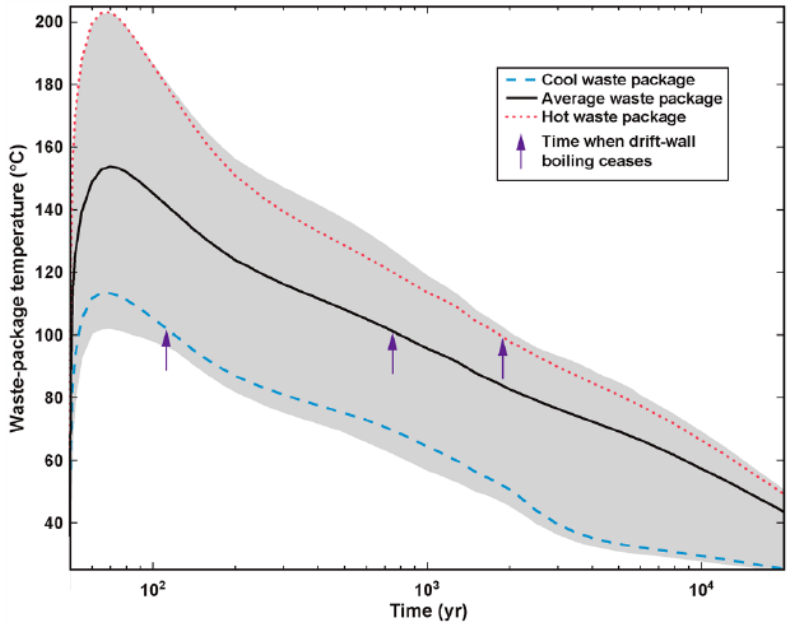

Figure 2-1. Range of Waste Package Temperature Versus Time (Sandia National Laboratory, 2007a)

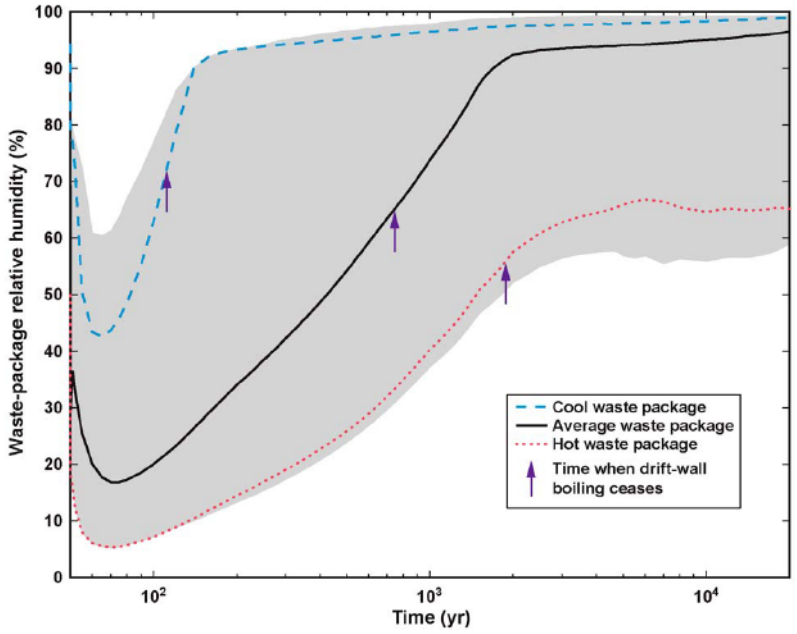

Figure 2-2. Range of Relative Humidity Versus Time (Sandia National Laboratory, 2007a)

water reactor waste package at the center of the repository (Sandia National Laboratories, 2007a). In Figure 2-1, the peak temperatures of the waste packages are predicted to be between 102 and 203 °C [216 and 398 °F]. The relative humidities reach minimum values when the temperatures are at peak values. As the temperature decreases, the relative humidity increases.

When the temperature of the drift wall is above boiling, liquid will not reach the drifts and seepage is not expected. Under these conditions, aqueous corrosion may still be possible by brines formed either through evaporation or by deliquescence of salts in dust deposited on the waste pack surfaces (Sandia National Laboratories, 2007b).

2.2 Thermodynamic Stability of Alloy 22 at 150 and 180 °C [302 and 356 °F]

The passive film stability was analyzed using a thermodynamic modeling software, titled Corrosion Analyzer™. The model used in this software is designed to provide a representation of chemical equilibria and thermophysical properties in the bulk solution and metal–solution interface thermodynamics. Thermodynamic stability diagrams were calculated for Alloy 22 at a given temperature and specific environment as discussed in the following paragraphs. Because Alloy 22 is composed of multiple elements, the software examines each of the major constituents of Alloy 22 and calculates the individual phases that can potentially be present in equilibrium with the solution for each element. It then creates individual pH-potential diagrams. Because the passive film consists mainly of nickel and chromium, the pH-potential diagrams for these two constituents were examined.

To examine how the passive film may change with temperature, Alloy 22 was modeled in simulated concentrated water at temperatures of 150 and 180 °C [302 and 356 °F]. The composition of simulated concentrated water was plugged into thermodynamic modeling software. A base metal of Alloy 22 was chosen from the software databanks, and the temperature was input. The results from the simplified system at 150 and 180 °C [302 and 356 °F] are shown in Figures 2-3 and 2-4, respectively. The blue-colored lines and compounds represent the nickel diagram, while the red-colored items represent chromium.

The results in Figure 2-3 indicate there is a large range where a chromium-rich oxide film would be thermodynamically stable. Above a pH of 5, the nickel is more thermodynamically stable as $NiCr_2O_4$. Similarly, the model shows that chromium is also more thermodynamically stable as Cr_2O_3 or $NiCr_2O_4$ depending upon the pH. At a pH below roughly 3.5, nickel is more stable in the aqueous state, while chromium would still be in a hydrated solid of $Cr_2(SO_4)_3 \bullet 14H_2O$. Below a pH of 5, the nickel is still in an aqueous state, while the chromium is in a Cr_2O_3 solid state. As the potential is increased in the low pH region, the chromium is calculated to oxidize from a +3 oxidation state to a +4 in CrO_2 and finally to a +6 in the aqueous $HCrO_4^-$. This is similar for the alkaline region, where chromium is initially maintained at a +3 oxidation state at lower potential, but oxidizes to +6 at higher potentials. The nickel phases described, however, are stable up to very high potentials.

The thermodynamic stability diagram at 180 °C [356 °F] is similar to the diagram at 150 °C [302 °F]. Most of the same species are still present, but the stability lines have been shifted for some species. For the nickel species, the region for $NiFe_2O_4$ has expanded in the mildly acidic region. In addition, the $NiFe_2O_4$ appears to have formed in the alkaline region. For the

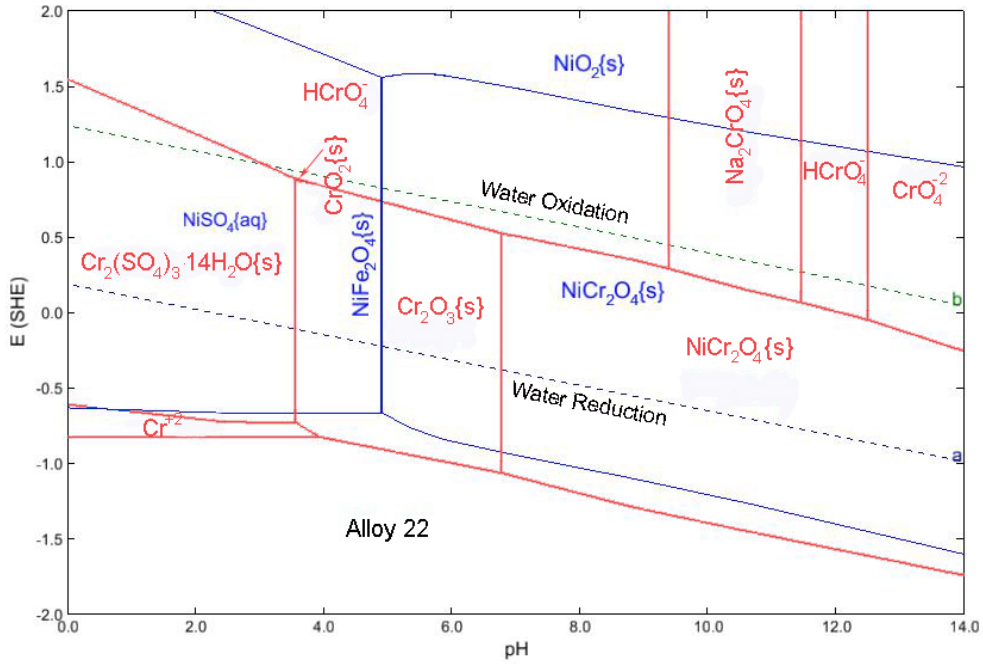

Figure 2-3. Calculated Potential-pH Diagram for Alloy 22 in Simulated Concentrated Water at 150 °C [302 °F] for Both Chromium and Nickel Species

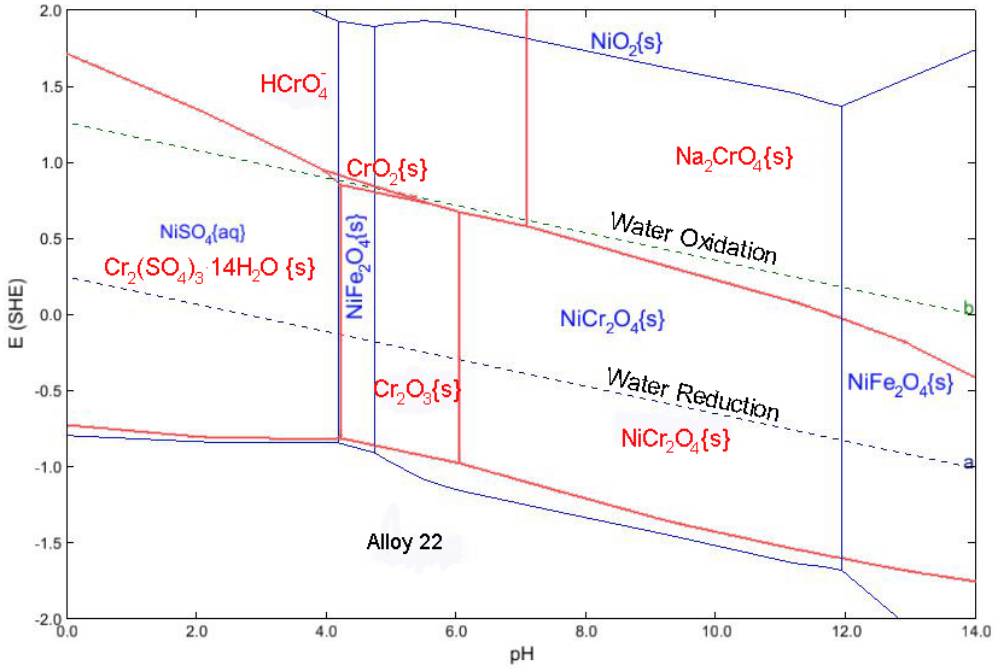

Figure 2-4. Calculated Potential-pH Diagram for Alloy 22 in Simulated Concentrated Water at 180 °C [356 °F] for Both Chromium and Nickel Species

chromium species, the Na_2CrO_4 compound has expanded into the more alkaline region and the Cr_2O_3 species is minimized in the acidic conditions, but most of the other conditions are the same.

The results from the thermodynamic modeling indicate that there is a large range of conditions at temperatures of 150–180 °C [302–356 °F] where a chromium-rich oxide is thermodynamically stable on the surface of Alloy 22. Only at very acidic or high potentials would a chromium-rich oxide be unstable.

2.3 Passive Film Characterization at Different Temperatures

To support the thermodynamic data from the previous section, experimental data from the available literature was examined. However, there is a limited amount of technical information on the passivity of Alloy 22 at elevated temperatures {>100 °C [>212 °F]}. Currently, most of the literature on the passive behavior of Alloy 22 at elevated temperatures comes from studies DOE sponsored as part of the Yucca Mountain program. Because there is a minimal amount of data in the open literature on the stability of the passive film on Alloy 22 at elevated temperatures, the properties of industrial analogs Alloys 600 and 690 were examined at elevated temperatures. Both Alloys 600 and 690 are nickel-based alloys with major additions of chromium and iron. The compositions for Alloys 600, 690 and 22 are provided in Table 2-1. Chromium is the main alloying addition that promotes passivity in these materials. The formation of a chromium (III)-rich passive film leads to the general corrosion resistance for these alloys. Choosing to evaluate Alloys 600 and 690 to understand the passive nature of Alloy 22 is appropriate because the chromium concentration in Alloys 600 and 690 envelops the chromium content of Alloy 22 and because these materials have been used in elevated temperature processes (e.g., nuclear reactor components).

Alloys 600 and 690 are high-temperature corrosion-resistant metals. They have been used to fabricate nuclear power plant components because of their limited passive corrosion susceptibility and mechanical properties. These materials are found throughout nuclear plants in steam generators, pressurized heater sleeves, and in the control rod drive mechanisms. They provide a good indication of the passive behavior of nickel-chromium-iron alloys in elevated temperature environment.

This section reviews the properties of the passive film on Alloy 22 at elevated temperatures by examining both the DOE data on Alloy 22 and industrial data on Alloys 600 and 690. Reviewing this information in conjunction with the data from the previous thermodynamic section will assist in evaluating the persistence of the passive film on Alloy 22.

Table 2-1. Chemical Composition of Candidate Material and Industrial Analogs

UNS* Designation	Weight Percent											
	Alloy	Fe†	Ni†	Cr†	Mo†	W†	Co†	Cu†	Mn†	Si†	C†	S†
N06022	22	2.0–6.0	Bal‡	20.0–22.5	12.5–14.5	2.5–3.5	2.5 max§	—	0.50 max	0.08 max	0.015 max	0.02 max
N06600	600	6.0–8.0	72.0 min§	14.00–17.00	—	—	—	0.50 max	1.00 max	0.75 max	0.10 max	0.015 max
N06690	690	7.0–11.0	58.0 min	27.0–31.0	—	—	—	0.50 max	0.50 max	0.50 max	0.05 max	0.015 max

*UNS—Unified Numbering System
†Fe—iron; Ni—nitrogen; Cr—chromium; Mo—molybdenum; W—tungsten; Co—cobalt; Cu—copper; Mn—manganese; Si—silicon; C—carbon; S—sulfur
‡Bal—balance
§max—maximum; min—minimum

2.3.1 Passive Film Properties of Alloy 22 at Elevated Temperatures

In a series of experiments by Orme, et al. (2004), autoclave tests were used to investigate the properties of Alloy 22 at temperatures above 120 °C [248 °F]. These experiments determined the influence of temperature and nitrate-to-chloride ratio on the corrosion rate of Alloy 22. The solutions studied included high ionic strength brines composed of Na^+, Cl^-, K^+, and NO_3^-. It was unclear from the report whether the system was held in a deaerated or aerated condition.

In these studies (Orme, et al., 2004), surface analysis techniques were used to characterize the composition of the oxide film. Several techniques were applied including X-ray Photoelectron Spectroscopy, Auger Electron Spectroscopy, Transmission Electron Microscopy, and Electron Energy Loss Spectroscopy. A discussion of the observed results follows.

X-ray photoelectron spectroscopy was used to determine the elemental composition along with a stoichiometric analysis. The surface analysis from the x-ray photoelectron spectroscopy indicated that the main contributions to the oxide film were from nickel [26–90 atomic percent (at%)] and chromium (3–40 at%). There were lower levels of molybdenum (0.1–9 at%) and iron (0.8–9 at%) in the oxide, while only trace levels of tungsten (<0.1–1.5 at%) were observed.

During this testing (Orme, et al., 2004), samples were held in both the vapor phase and the liquid solution. In most of the tests, the sample held in vapor contained more molybdenum oxide than the liquid-immersed samples. Another difference that was observed between the vapor and liquid-immersed samples was the change in nickel-to-chromium concentration with aging time. In the liquid phase, the nickel-to-chromium concentration decreased, while in the vapor phase it increased. These differences between the vapor and liquid phases were thought to occur because in liquid solution, the samples are reacting with a large volume of water, while the samples in vapor are reacting with a thin film of fluid. Orme, et al. (2004) hypothesized that the results were due to a change in the dissolution kinetics. In the liquid phase, dissolution is much faster than the vapor phase. The nickel-to-chromium ratio increases in vapor samples because the nickel cannot dissolve as easily as in the immersed condition. Similarly, molybdenum had a higher relative concentration on the surface of the sample held in the vapor phase compared to samples immersed in the liquid phase. This was also believed to be related to the difference in the dissolution kinetics associated with the different environmental conditions.

In the same study, Orme, et al. (2004) examined the speciation of chromium by curve fitting the x-ray photoelectron spectroscopy data to four different oxidation states [i.e., 0 for metal; +3 for Cr_2O_3, $Cr(OH)_3$, or CrOOH; +4 for CrO_2; and +6 for CrO_3]. The chromium in the oxide film was predominantly in the +3 oxidation state. Two samples from the test with the combination of highest nitrate-to-chloride ratio (6.7) and high temperature {160 °C [320 °F]} showed different results. In this environment, both the vapor- and liquid-tested samples indicated that chromium was predominantly in the +6 oxidation state. It was suggested that combining high temperatures with high chloride-to-nitrate ratio may accelerate the metal oxidation.

In addition to the x-ray photoelectron spectroscopy analysis, the surface oxide was investigated using cross-sectional transmission electron microscopy. This technique was evaluated along with Auger electron spectroscopy depth profiling. Orme, et al. (2004) indicated that in the low nitrate-to-chloride ratio (0.05) and at 140 °C [284 °F], a smooth oxide grows on the surface of the metal. Over time, this oxide became less porous. The thickness of this oxide varies from roughly 0–60 nm [0–2.36×10^{-3} mils]. The Auger profile indicated that these samples predominantly are composed of nickel, chromium, and oxygen.

Samples in higher nitrate-to-chloride ratio (0.5) and temperature of 140 °C [284 °F] appeared similar to the ones previously discussed. The oxide was thinner but was still smooth and was mainly composed of nickel, chromium, iron, and molybdenum. When the temperature was increased to 120 °C [248 °F] and the nitrate-to-chloride ratio was kept high (0.3), the oxide film was quite different. The base metal was no longer smooth and appeared to have corroded. The oxide was much thicker and was stratified. There was an outer polycrystalline layer that appeared to be $Ni(OH)_2$. However, there was still the indication of a chromium-rich oxide layer from electron energy loss spectroscopy.

In another study, Dixit, et al. (2006) expanded experimental testing to higher nitrate-to-chloride ratios and higher temperatures. Alloy 22 was examined in nitrate-to-chloride ratios of 7.4 at 160 °C [320 °F] and nitrate-to-chloride ratios of 7.4 and 0.5 at 220 °C [428 °F]. Testing was conducted in an autoclave containing a solution of Na^+, Cl^-, K^+, and NO_3^- that had been purged with nitrogen gas. After purging the autoclave, it was brought up to temperature and pressure and held for 9 months. The oxide layers were examined with both x-ray photoelectron spectroscopy and auger electron spectroscopy.

The analysis of the surface oxide from this testing (Dixit, et al., 2006) revealed that for both the vapor and liquid phase samples, the oxide outer layer consisted mainly of aluminum hydroxide, some silicates, and an alloy oxide enriched in nickel relative to chromium and molybdenum compared to the base metal. The liquid-tested sample had a much thicker oxide layer compared to the vapor sample.

On the liquid-tested sample, the x-ray photoelectron spectroscopy data indicated that an outer oxide consisted mainly of $Ni(OH)_2$ with some amounts of chromium oxide. Because of thick aluminum and silicon coatings on the surface, the oxidation state of the chromium was not distinguishable. There was a nickel-enriched outer layer on the surface of the Alloy 22 in the liquid environment identified from the Auger analysis. However, the Auger electron spectroscopy did not indicate any specific chromium-enriched layer.

The samples held in the vapor phase from this testing (Dixit, et al., 2006) were similar to those in the liquid. The surface oxide was primarily composed of $Ni(OH)_2$ with minor amounts of chromium oxides. Chromium (+3) and Chromium (+4) were the primary types of chromium, with minor amounts of Cr (+6). Minor amounts of chromium were detected in the oxide film because most of the chromium oxidized to +6 and dissolved to the solution. Therefore, only the remaining chromium observed in the oxide film was in the +3 or +4 state. Chromium metal was only detected at temperatures below 160 °C [320 °F], which may indicate a thick oxide layer at higher temperatures. The Auger electron spectroscopy depth profiling indicated that there was a nickel-rich outer oxide for all the samples. There was also an indication of an inner chromium-rich oxide on the Alloy 22 sample held at 160 °C [320 °F] with a nitrate-to-chloride ratio of 7.4 and the sample held at 220 °C [428 °F] with a nitrate-to-chloride ratio of 0.5. The sample that was held at 220 °C [428 °F] with a nitrate-to-chloride ratio of 7.4 did not indicate a chromium-rich inner oxide.

2.3.2 Industrial Analogs

As previously mentioned, Alloys 600 and 690 are nickel-based alloys containing chromium that envelop the chromium concentration found in Alloy 22. Both Alloys 600 and 690 have been examined at elevated temperature due to their use in nuclear power plants. Because the

passive attributes of Alloy 22 are associated with its chromium content, the corrosion behavior of Alloys 600 and 690 at elevated temperatures provides insight to similar reactions with Alloy 22.

In a study Montemor, et al. (2003) conducted, Alloys 600 and 690 were examined at high temperature {320 °C [608 °F]} and various pH conditions by Auger electron spectroscopy. The test solutions contained sodium hydroxide and sodium sulfate to create various pH conditions including 5, 8, and 10. The Auger electron spectroscopy analysis indicated that for both Alloys 600 and 690 in the pH 5 solution, there was a thin outer oxide film covered by an inner chromium-rich oxide layer. When the pH was increased to 8, the chromium content decreased in both outer and inner films. The results indicated that there was an iron/nickel-rich outer oxide. While the overall chromium content decreased in both films, there continued to be an inner chromium-rich oxide on both alloys. When the solution pH increased to 10, the chromium oxide concentration decreased again in both outer and inner films. While the outer film was still composed of nickel and iron oxides, it was difficult to discern any inner chromium-rich oxides.

Hur and Park (2006) evaluated the effect of temperature on the passive film characteristics of Alloy 600. Alloy 600 was examined in deaerated 0.282 M sodium chloride solution between the temperatures of 90 and 280 °C [194 and 536 °F]. X-ray photoelectron spectroscopy was used to examine the oxide film that formed. At 90 °C [194 °F], the chromium species detected included a metallic Cr and Cr +3 oxidation state. The nickel species detected included metallic nickel and a Ni +2 oxidation state. The nickel peak intensities were very weak compared to the chromium signals. When the temperature was increased to 280 °C [536 °F], the metallic species were no longer observed. This was likely due to the increased thickness of the film. While chromium hydroxide/oxide was the major species at 90 °C [194 °F], the nickel hydroxide/oxide intensity increased with temperature. In addition, the oxygen peaks shifted to indicate an increased concentration of oxide at 280 °C [536 °F] rather than bound water or hydroxide. The chromium species at the higher temperature still included Cr in the +3 oxidation state. There was no discussion in Hur and Park (2006) about the presence of a Cr +6 oxidation state.

Mintz and Devine (2004) examined Alloy 600 in 288 °C [550 °F] solution containing 2 ppm LiOH and 1,200 ppm H_3BO_3. Alloy 600 was examined by both surface enhanced Raman spectroscopy and Auger electron spectroscopy. The Alloy 600 samples were polarized from a low electrochemical potential (−1,600 mV versus standard hydrogen electrode) to −100 mV versus standard hydrogen electrode. The results indicated that at lower potentials, the oxide initially formed a chromium-rich M_3O_4 type of film. The M stands for mixed metal (i.e., nickel, chromium, and iron). As the potential increased, the subsequent oxides that formed included NiO, $(Fe, Cr)_2O_3$, and $Ni_{3-x}Fe_xO4$.

2.4 Assessment of the Film Stability of Alloy 22 at Elevated Temperatures in the Potential Repository Environment

Thermodynamic modeling of Alloy 22 in simulated concentrated water at temperatures of 150 and 180 °C [302 and 356 °F] was conducted to determine the passive film stability. The pH-potential diagrams that were constructed for the environment described showed a large region of stability for either Cr_2O_3 and/or $NiCr_2O_4$. Both of these compounds contain chromium in the +3 state, which is consistent with the experimental evidence. Only at very high potentials or low pH did thermodynamic instability occur for the oxide film.

The long-term stability of the passive film indicated by the thermodynamic data is difficult to assess by comparison to short-term tests. However, the results of the 9-month autoclave tests Orme, et al. (2004) conducted on Alloy 22 in NaCl-$NaNO_3$-KNO_3 solutions at elevated temperatures {120–220 °C [248–428 °F]} indicated that a chromium-rich oxide film was present in most of the testing. This chromium oxide consisted mainly of a +3 oxidation state. This would tend to be either Cr_2O_3, $Cr(OH)_3$, CrOOH, or possibly $NiCr_2O_4$. This is consistent with the thermodynamic data, where chromium is mainly stable in a +3 oxidation state. It was not until the temperature was much higher {i.e., at least 160 °C [320 °F]} and the nitrate-to-chloride ratio was high (around 6.7) that the chromium oxidize reached a +6 state, which would be expected to more readily dissolve.

Because there is a minimal amount of operational data in the literature on the stability of the passive film on Alloy 22 at elevated temperatures, analog materials were examined to aid in the evaluation. Two materials evaluated were Alloys 600 and 690. These two materials were chosen because of chromium concentration similar to Alloy 22 and because they have been used in elevated temperature processes (e.g., nuclear reactor components). Studies of these analog materials have been conducted at temperatures exceeding 320 °C [608 °F]. The results from the data examined reveal that a passive chromium-rich oxide can form at elevated temperatures in solutions ranging in pH from 5 to 10.

Based on the thermodynamic modeling results and short-term experimental literature results, a chromium-rich oxide passive film is expected to be stable at elevated temperatures. There are no clear degradation mechanisms that were observed to interfere with the stability of the passive film in the short-term experiments. However, if mechanisms require long initiation times, such degradation mechanisms would be difficult to detect. An example of a degradation mechanism with a potentially long initiation time is sulfur segregation, which is described in Chapter 3.